

Reducing noise from a Stirling micro cooler used with an InSb diode

Nicolas R. Bingham and Michael C. B. Ashley*

School of Physics, University of New South Wales, Sydney NSW 2052, Australia

ABSTRACT

Stirling micro coolers, such as the K508 from Ricor, are useful components of scientific instruments when there is a need to remove modest amounts of heat ($\sim 1/2$ W) at liquid nitrogen temperatures with an input power of less than 10 W. The action of the cooler can, however, couple noise into sensitive detectors through a variety of mechanisms such as electromagnetic interference, mechanical vibration, and small temperature fluctuations. We report on successful noise-mitigation strategies for our application, an InSb diode for detecting light at 2.4 microns. The largest benefit was obtained by synchronizing the integration times with the position of the piston in the micro cooler. The piston position was determined using a hall-effect rotor position sensor in the driving motor.

Keywords: InSb diode, Stirling-cycle micro cooler, infrared detector, charge-integrating preamplifier, noise reduction, Antarctica

1. INTRODUCTION

We are building an instrument using an InSb diode cooled to 77K to measure the sky background at 2.4 microns in Antarctica. Due to a combination of high altitude, dry atmosphere, low temperature, and stable conditions, sites on the Antarctic plateau offer some of the best conditions on earth for infrared astronomy.¹ The astronomical K-dark band at 2.4 microns in particular has exceptionally low sky emission—about one-hundredth the flux as observed from Mauna Kea Observatory, making the measurement quite challenging. The instrument will be at a remote, unmanned site without access to liquid cryogenics, making it necessary to use a low-power cooler such as a Ricor Stirling micro cooler.

The instrument is based on a single InSb diode with a cold band-pass filter, making it sensitive to sky spectral emission at 2.38 ± 0.08 microns.² An external short-pass filter eliminates a small long-wavelength leak from the band-pass filter. The infrared detector is attached to the cold head of a Ricor K508 micro cooler, shown in Figure 1. In operation, a differential measurement is made by optically chopping between two 4 degree field-of-view beams angularly separated by 45 degrees on the sky.³ The resultant signal at the chopper frequency is proportional to the difference in emission from the atmosphere at two air-masses. From this measurement we can calculate the absolute sky emission scaled to one airmass in the K-dark band.⁴

In our instrument, the only part of the electronics that is cooled is the InSb diode. Photocurrents measured in picoamps need to be transferred from within the cooler envelope to the preamplifier and associated circuitry. Great care needs to be taken with the preamplifier design, wiring layout and grounding, to minimize the various noise sources. Tiny changes to the environment, such as opening or closing one side of the shielded case of the instrument, loosening screws which affect the case-to-earth impedance, or the presence/absence of a toothed lock washer (which affects the cooler-to-case impedance) are all immediately obvious from the data.

Stirling micro coolers can introduce noise in a number of ways, e.g., electrical noise from the motor commutation or pulse-width modulation (PWM) switching, magnetic interference from the stator windings or rotor magnets, thermal cycling at the cold head, and vibration.

Operation of the micro cooler results in significant electrical noise at two frequencies: brushless motor commutation at about 450 Hz, and PWM switching at about 60 kHz. For exceptionally low-noise applications, linear

* m.ashley@unsw.edu.au; phone +61 2 9385 5465

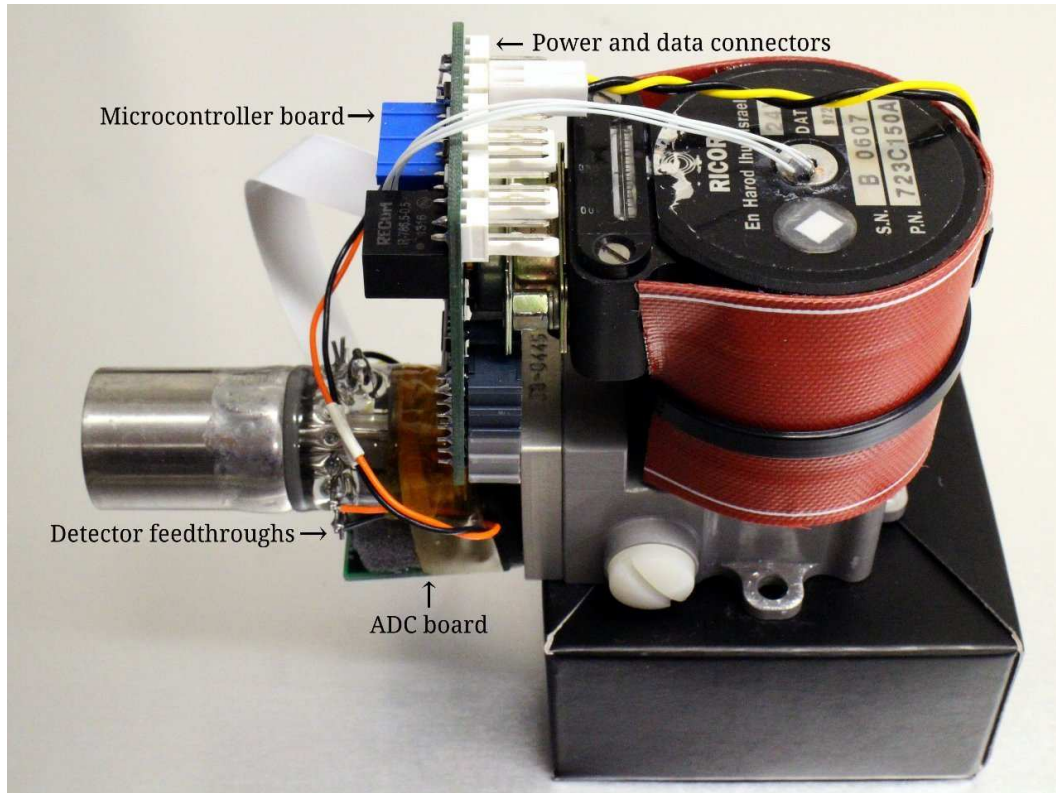


Figure 1. The Ricor K508 micro cooler with attached microprocessor and ADC boards linked by a flexible flat cable (FFC). The ADC board is soldered directly to the feedthroughs from the glass envelope of the cooler, to minimize wiring loops. The FFC carries only digital signals between the microprocessor and ADC boards.

mode (as opposed to PWM-type) motor controllers are available, and more advanced motor controllers use sinusoidal current control (rather than trapezoidal or six-step commutation). Either of these operating modes would reduce the radiated electrical noise, but neither are applicable to the “Hybrid 10” controller used in our early model of Ricor K508 micro cooler.

2. THE ORIGINAL INSTRUMENT

The original version of the instrument dating from the early 2000s used a mechanical chopper wheel alternating the detector signal between the two beam paths at 77 Hz. The photocurrent was sent to a transimpedance preamplifier, and the differential signal was passed through a high-Q analog filter at 77 Hz and additional amplification before 14-bit analog-to-digital conversion.

In this original configuration, the instrument performance was theoretically limited by Johnson noise in the transimpedance amplifier feedback resistor. In practice, we had larger noise contributions from ground loops, EMI from the cooler motor commutation and switching, EMI from the chopper wheel position sensor signal, and microphonics.

3. IMPROVEMENTS TO THE SIGNAL CHAIN

In the original instrument, a digital signal was transmitted from an optical position sensor on the chopper wheel to be used for chopper motor speed feedback and lock-in amplifier synchronization. The wires from this signal had to pass close to the InSb detector, due to the mechanical design of the instrument. Despite shielding and careful grounding, this signal induced small currents in the detector signal loop. This noise source was particularly detrimental to the measurement since its effects were exactly in phase with the chopped sky signal.

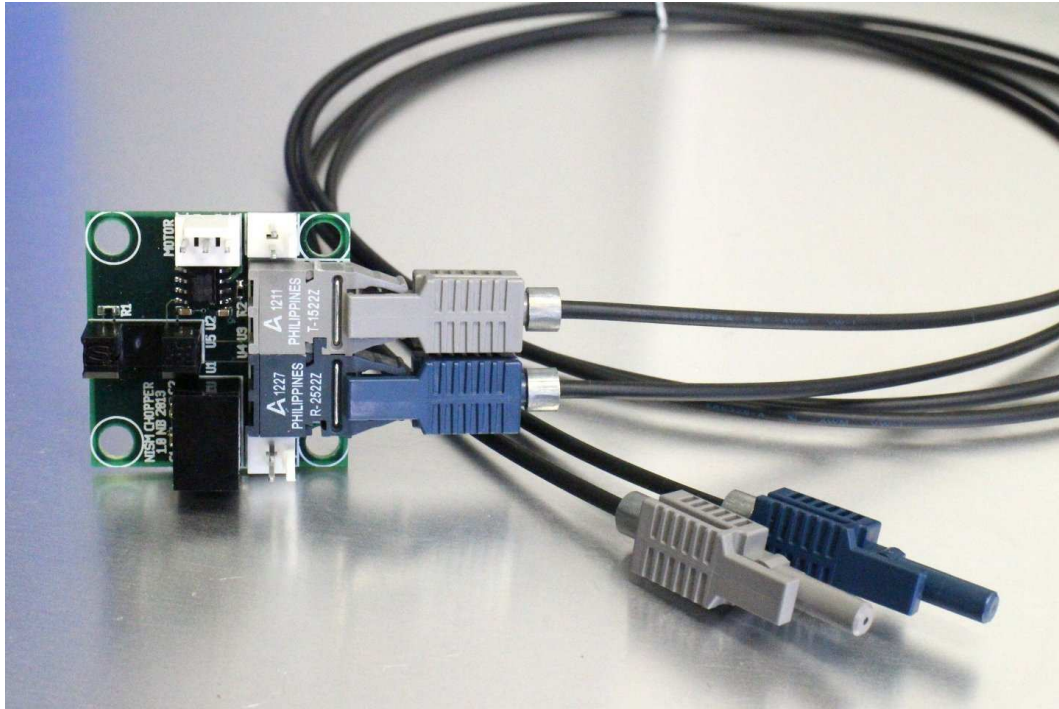


Figure 2. The chopper motor controller and feedback board, with fiber optic cables and connectors.

By transmitting this signal with an inexpensive plastic fiber optic (Avago Versatile Link), this noise source was eliminated. The chopper motor controller and feedback board is shown in Figure 2.

We then replaced the transimpedance preamplifier with a Texas Instruments DDC112 charge-integrating preamplifier with on-chip 20-bit ADC (shown in Figure 3). This eliminates Johnson noise, although it introduces noise from charge injection when switching the capacitors in the integration circuit. The charge-integrating ADC arrangement means that performance is now limited by detector signal noise accumulated during the integration period, and inherent detector $1/f$ noise over longer time scales. The most important advantage of the DDC112, however, is that it allows a compact circuit design that gives a digital output signal within a centimetre or two of the InSb detector. The loop area of the detector signal is as small as is practical, and it is constructed from rigid materials to limit movement or changes in loop area resulting from vibration. This significantly reduced the opportunity for noise pickup in the wiring, and from microphonics. Analog-digital conversion is performed on-chip, eliminating the downstream filter, amplification, and separate ADC, all of which were points at which noise could enter the system. Also, by eliminating the analog filter, we have the flexibility to easily change the chopper frequency under microprocessor control.

4. DATA ACQUISITION DESIGN

The DDC112 analog-digital conversion results are read using an Atmel AVR 8-bit microcontroller which also controls the micro cooler, various heaters and other instrument-specific features. The microcontroller is powerful enough to perform basic averaging and digital filtering on-chip, and a Modbus interface enables every sample to be polled by a host computer for detailed analysis. A real-time plotting tool created using Python and Matplotlib was invaluable in the process of identifying and resolving many noise sources.

Our control software also enables us to record data whilst sweeping the integration frequency over a wide range, which is useful to identify the frequency of noise sources which would otherwise only present as aliasing artifacts.

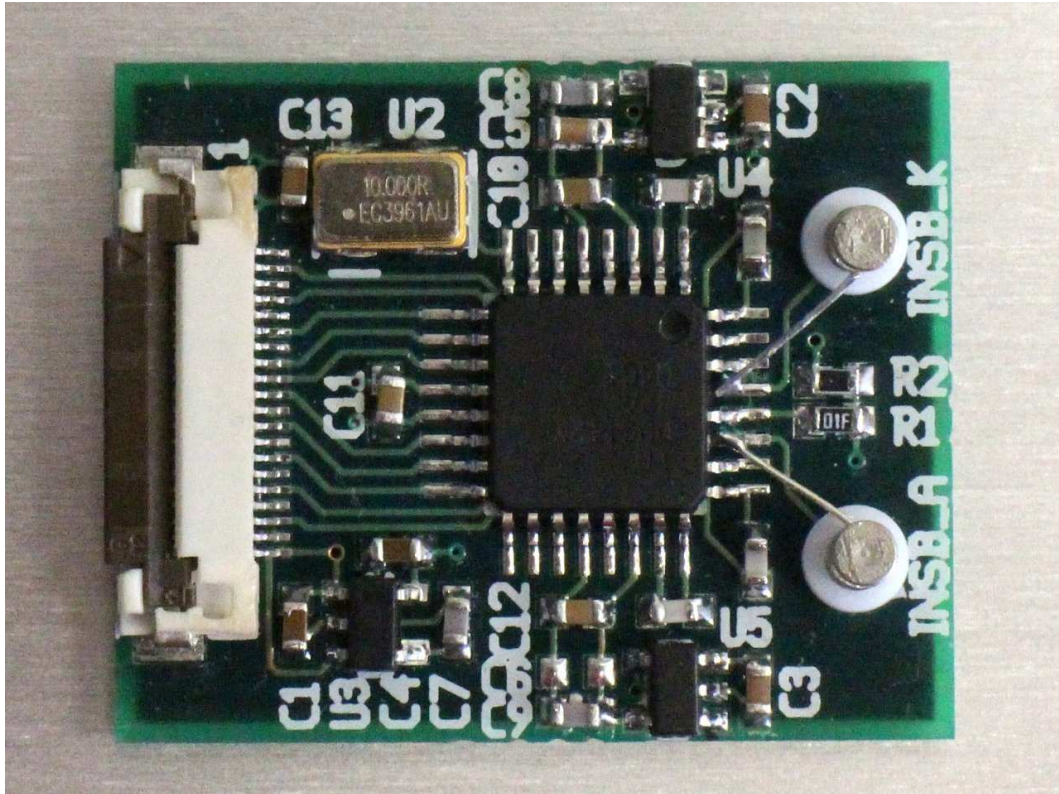


Figure 3. The DDC112-based charge-integrating ADC board. Care is required in the circuit layout to avoid ground loops and leakage currents. Of particular note, the input pins to the DDC112 chip have been lifted from the board and air-wired to PTFE-insulated terminals, which are soldered directly to the detector feedthroughs. This prevents significant leakage currents on the surface of the circuit board which could occur due to humidity or contamination.

5. NOISE AT THE PISTON FREQUENCY

The remaining issue was a close-to-sinusoidal modulation of the apparent InSb photocurrent at the Stirling engine piston frequency (half the frequency of the motor current waveform), at about 25 Hz. In the K508, the piston frequency varies with the desired operating temperature and the thermal load on the cold head, in such a way as to stabilize the detector temperature (in practice, the forward voltage drop of a nearby silicon diode is used as a proxy for the detector temperature). Hence it is not possible to synchronise the piston to a fixed frequency, without causing the detector temperature to drift.

To investigate the noise at the piston frequency we initially derived the piston position using the current waveform from the brushless DC motor that drives it. We used a current transducer and digitizing the current waveform, followed by a real-time FIR digital filter and thresholding to determine the position of each motor commutation. An example of the motor current waveform and commutation periods identified by edge detection is shown in Figure 4.

By starting/stopping the detector signal integration at known points relative to the derived piston position, we were able to map out the modulation over a full cycle. These experiments showed that the modulation was at the piston frequency, not at the motor DC supply or winding current frequency, which rules out electrical and magnetic coupling from the motor. Also, the modulation was smooth, with no glitches corresponding to motor commutation. Finally, the modulation was additive, as opposed to multiplicative, in the detector output, which eliminated possible causes such as cyclic variations in the sensitivity of the detector. The amplitude of the modulation was independent of the signal measured by the detector.

Our best guess at this point is that the modulation is caused by cyclical changes in the cold-head temperature

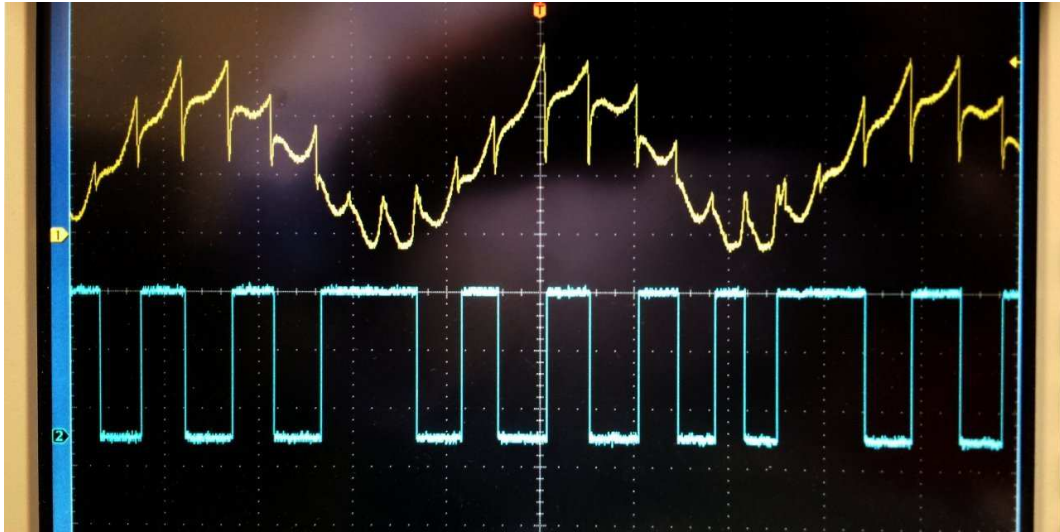


Figure 4. A plot of the motor current (upper, yellow) and commutation periods (lower, blue) identified by edge detection. Note that the motor current passes through two maximums for one cycle of the piston: one maximum corresponds to the piston being pushed, and the other to the piston being pulled. There are 18 commutation edges per piston cycle.

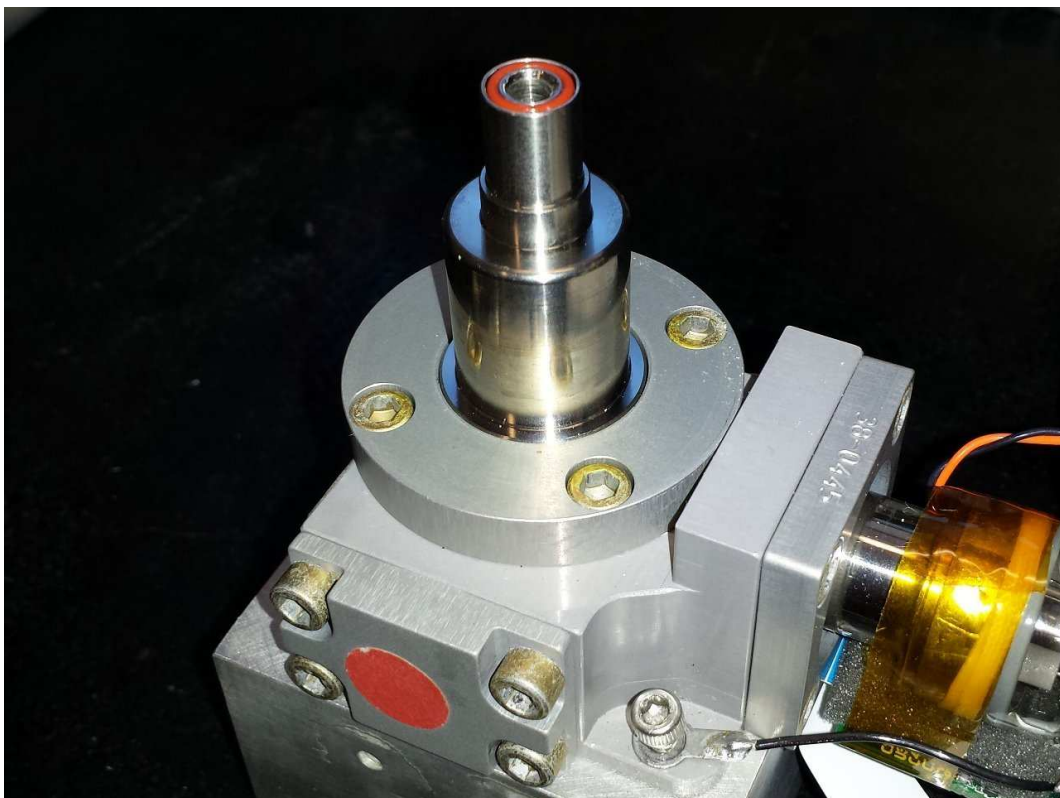


Figure 5. The K508 micro cooler with the stator windings removed. The rotor is within a stainless steel case and is magnetically coupled through a hermetic seal.



Figure 6. Inside the micro cooler motor stator. The blue wire at the center of the image was added to make contact with one of three hall sensors embedded in epoxy, in order to provide a readout of the rotor position.

as the piston moves, resulting in small currents, possibly as a result of thermocouple effects in the wires connecting the detector to the feedthroughs.

Synchronizing to the piston produced a drop in the sample standard deviation from 2000 to 35 ADU.

The remaining practical issue was the complexity of using the current waveform to derive the piston position. The nature of the Stirling-cycle cooler means that the torque and the six-step commutation periods are non-uniform throughout each motor revolution. This, as well as phase delay introduced by the current transducer and digital filter make the edge detection technique quite complicated. Also, dependence on predetermined windowing constants means that this technique cannot easily tolerate significant micro cooler speed variation.

Fortunately, it was relatively straightforward to access the stator of the K508 by removing the central screw from the top of the cooler. The rotor is magnetically coupled through a hermetic seal, as shown in Figure 5. The rotor position sensors are embedded in the same epoxy used to encapsulate the stator windings, but can be accessed by carefully grinding or melting away this material as shown in Figure 6. We connected one of the three hall sensors to an unused pin on the DB-9 connector of the K508, to make its signal accessible to our microcontroller board.

Figure 7 shows the motor current waveform and the rotor position as a function of the hall-effect position sensor. Synchronization of the integration period using this technique has proven to be reliable over a very wide range of micro cooler operating speeds.

In bench tests with a room-temperature source, these improvements have collectively increased the measurement signal-to-noise ratio from less than 50 to over 2000. Though the expected sky signal is several orders of magnitude lower than that of our room-temperature source, we are confident that the updated instrument will greatly improve the quality of data we are able to record when it is deployed to Antarctica later this year.

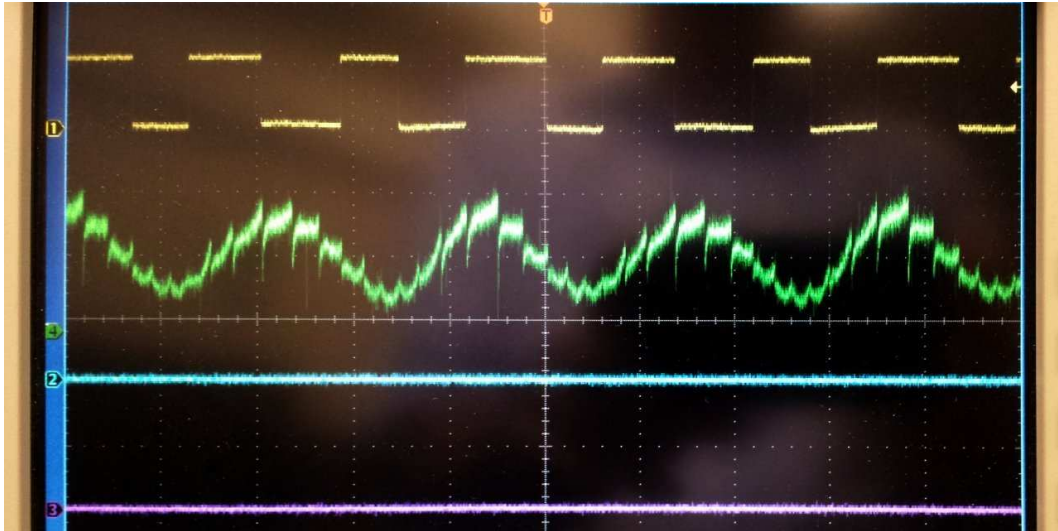


Figure 7. A plot of the motor current (lower, green) and rotor position (upper, yellow) measured by the hall-effect position sensor. Note that the upper trace toggles with each hall edge. The hall sensor is triggered six times per piston cycle. Close inspection shows that the motor current waveform is slightly different in the two halves of the piston cycle.

ACKNOWLEDGMENTS

We are grateful to Ricor for providing helpful advice during our investigations. This project is partly funded by the Australian Government, being conducted as part of the Super Science Initiative, financed from the Education Investment Fund, and administered by Astronomy Australia Limited.

REFERENCES

- [1] Ashley, M. C. B., "Site characteristics of the high antarctic plateau," *IAU Symposium*, **288**, 15–24 (2013).
- [2] Storey, J. W. V., Ashley, M. C. B., and Burton, M. G., "Novel instruments for site characterization," *Proc. SPIE*, **4008**, 1376–1382 (2000).
- [3] Lawrence, J. S., Ashley, M. C. B., Burton, M. G., Calisse, P. G., Everett, J. R., Pernic, R. J., Phillips, A., and Storey, J. W. V., "Operation of the near infrared sky monitor at the south pole," *Publ. Astron. Soc. Aust.*, **19**, 328–336 (2002).
- [4] Lawrence, J. S., Ashley, M. C. B., Burton, M. G., and Storey, J. W. V., "Observations of the antarctic infrared sky spectral brightness," *Proc. SPIE*, **4836**, 176–179 (2002).